

# Meta-Learning Mini-Batch Risk Functionals

Jacob Tyo<sup>1,2</sup> Zachary C. Lipton<sup>2</sup>

## Abstract

Supervised learning typically optimizes the expected value risk functional of the loss, but in many cases, we want to optimize for other risk functionals. In full-batch gradient descent, this is done by taking gradients of a risk functional of interest, such as the Conditional Value at Risk (CVaR) which ignores some quantile of extreme losses. However, deep learning must almost always use mini-batch gradient descent, and lack of unbiased estimators of various risk functionals make the right optimization procedure unclear. In this work, we introduce a meta-learning-based method of learning an interpretable mini-batch risk functional during model training, in a single shot. When optimizing for various risk functionals, the learned mini-batch risk functions lead to risk reduction of up to 10% over hand-engineered mini-batch risk functionals. Then in a setting where the right risk functional is unknown a priori, our method improves over baseline by 14% relative ( $\sim 9\%$  absolute). We analyze the learned mini-batch risk functionals at different points through training, and find that they learn a curriculum (including warm-up periods), and that their final form can be surprisingly different from the underlying risk functional that they optimize for.

## 1. Introduction

The standard supervised learning procedure for training neural network models is to perform mini-batch gradient descent, where a model is presented with a small subset of data (mini-batch) and the model is updated with gradients derived from its outputs on that mini-batch. Typically, we want to minimize the expected value of the loss, in which case, using the expected value of the mini-batch loss is a clear choice. By the linearity of expectation, the gradient

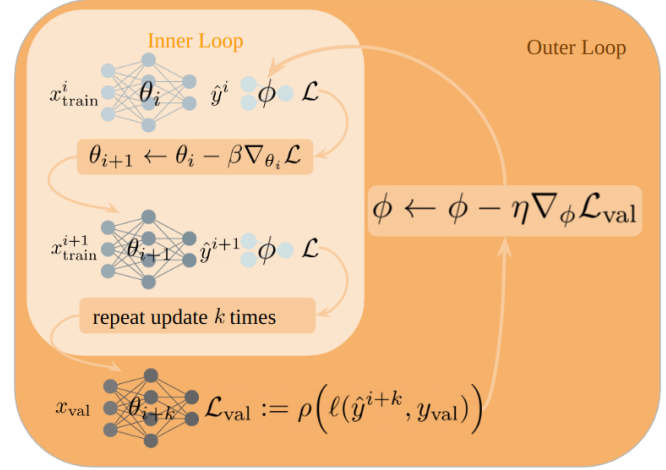


Figure 1. A high-level description of our meta-learning procedure. Given a model parameterized by  $\theta$ , this procedure learns a mini-batch risk functional, parameterized by  $\phi$ , that is a convex combination of the mini-batch losses. Trained in a single shot alongside the model, the learned mini-batch risk functional provides a means of better optimizing for dataset risk functionals of interest ( $\rho$ ) and can be used to automatically detect and deal with some forms of distribution shift.

of the mini-batch is an unbiased estimator of the gradient of the dataset. However, we are often in responsible decision-making settings such as healthcare (Patel et al., 2019; Rajpurkar et al., 2020; Tschandl et al., 2020), credit lending (Bussmann et al., 2021; Kruppa et al., 2013), and employment (Raghavan et al., 2020; Hoffman et al., 2018), where risk factors make optimizing for the expected value of the loss undesirable. Instead, we often want to optimize for risk functionals such as the Inverted Conditional Value at Risk (ICVaR), which ignores a percentage of the highest loss samples, or the trimmed risk, which ignores extreme high and low loss samples. In such cases, a mini-batch risk functional that produces unbiased gradients of the dataset risk functional is not available.

This is the first setting we focus on: determining the right mini-batch risk functionals to use for the optimization of various dataset risk functionals. But we also study a second, more challenging setting, where given a problem where a risk functional could be useful but is *unknown* a priori, can we meta-learn the right mini-batch risk functional for

\*Equal contribution <sup>1</sup>DEVCOM Army Research Laboratory, Maryland, USA <sup>2</sup>Machine Learning Department, Carnegie Mellon University, Pittsburgh, USA. Correspondence to: Jacob Tyo <jacob.p.tyo.civ@army.mil>.

maximum performance?

In this paper, we introduce a meta-learning-based method of learning an interpretable mini-batch risk functional during model training, in a single shot, that is effective in both aforementioned settings. When optimizing for various risk functionals, the learned mini-batch risk functions lead to risk reduction of up to 10% over hand-engineered mini-batch risk functions. Then in the presence of label noise, where risk functionals can be useful but the right one is unknown, our method improves over baseline by over 14% relative ( $\sim 9\%$  absolute) among 50% random labels, even when given *no* noise-free data. Our learned mini-batch risk functions are restricted to taking a convex combination of mini-batch loss quantiles, and are therefore clearly interpretable. We analyze the learned mini-batch risk functionals at different points through training, and find that they learn curriculums (including warm-up periods), and that their final form can be surprisingly different from the underlying risk functional that they are optimizing for.

Our core contributions are:

- meta-learning-based method for learning an interpretable mini-batch risk functional, in a single shot
- empirical study revealing that our learned mini-batch risk functionals better optimize for risk functionals of interest, reducing risk by up to 10%
- experimental demonstration that our learned mini-batch risk functionals can learn effective functionals even when a useful hand-crafted risk function is unknown a priori, improving over baseline by 14% relative ( $\sim 9\%$  absolute) among 50% random labels
- analysis of the learned mini-batch risk functionals revealing their surprising difference from hand-crafted risk functionals, and interesting dynamics such as automatic curriculum development.

## 2. Risk Sensitive Learning

First, we setup the problem of risk-sensitive learning. Specifically, given training data  $\{X_i, Y_i\}_{i=1}^n$  comprising the dataset  $\mathbb{D}_{\text{train}}$  (which is drawn from the distribution  $\mathbb{P}_{\text{train}}$ ) where  $C$  is the number of classes,  $b$  is the batch size,  $d$  is the dimensionality of the input,  $X \in \mathcal{X} \subseteq \mathbb{R}^d$  and  $Y \in \mathcal{Y} \subseteq \mathbb{R}^C$ , a loss function  $\ell : \mathcal{Y} \times \mathcal{Y} \rightarrow \mathbb{R}^C$ , a risk functional  $\rho : \mathbb{R}^b \rightarrow \mathbb{R}$  maps a loss distribution to a real value, and a hypothesis class  $\Theta$ , risk-sensitive learning optimizes for

$$\theta^* \in \arg \min_{\theta \in \Theta} \rho(\ell_{f_\theta}(X, Y)), \quad (1)$$

where  $\ell_{f_\theta}(X, Y) := \ell(f_\theta(X), Y)$  is the loss under model  $f$  parameterized by  $\theta$ . Furthermore, we will use  $X_{\text{train}}$ ,

$Y_{\text{train}}$  and  $X_{\text{val}}, Y_{\text{val}}$  to represent mini-batches of training and validation data respectively.

This formulation encapsulates traditional learning, in which case the risk functional is set to be the expected value:  $\rho = \mathbb{E}$ . Risk-sensitive learning explores the use of different risk functionals  $\rho$ , whether for training models when all samples should *not* be treated equally (i.e. fairness, dangerous actions, etc.), or to address specific types of distribution shifts. Table 1 details common risk functionals along with their formal definition and interpretation. Table 2 enumerates common types of distribution shifts.

## 3. Learning Risk Functionals

As a final note before introducing our method in detail, our method requires two datasets during training. We use the terms training, validation, hyper-validation, and test to refer to each of the dataset splits. Specifically, given a train and a test set, we split the train set into a train, a validation, and a hyper-validation set randomly as 90%/5%/5% of the original train set, leaving the test set unaltered. From this point on, when the validation data is mentioned, we are referring to that specific split of the training data. For hyperparameter selection, we leverage the hyper-validation set.

In this work, we propose a method to automatically learn mini-batch risk functionals, directly from data, based on a MAML-like (Finn et al., 2017) meta-learning formulation. Specifically, the mini-batch risk functional  $g_\phi$  is implemented as a linear layer, restricted to taking a convex combination of mini-batch loss quantiles. We make no assumption on the form of the model  $f$ , other than to assume that it is parameterized by some parameter vector  $\theta$ , and that gradient-based learning techniques can be used. To optimize  $g_\phi$ , we first set  $\theta' = \theta$  and then repeat the following update for some number of *inner steps*

$$\theta' \leftarrow \theta' - \beta \nabla_{\theta'} g_\phi(\ell_{f_{\theta'}}(X_{\text{train}}, Y_{\text{train}})), \quad (2)$$

where  $\beta$  is the inner learning rate, resulting in an updated  $f_{\theta'}$ . We then take an *outer step* by passing a mini-batch of validation data through  $f_{\theta'}$ , and then differentiating through this entire process with respect to  $\phi$ . Therefore, the update for  $\phi$  is:

$$\phi \leftarrow \phi - \eta \nabla_\phi \rho(\ell_{f_{\theta'}}(X_{\text{val}}, Y_{\text{val}})). \quad (3)$$

Notice that this update only depends on  $\phi$  via the derivation of  $\theta'$ , which is critical in preventing degenerate gradients. If gradients of  $\phi$  are calculated in the inner steps, or if calculated after a single update, then  $\phi$  can push the loss arbitrarily low, regardless of model output. Finally, to complete this outer step and continue training, the model parameters are reset to  $\theta$ , a new mini-batch of training data is drawn,

Table 1. Definitions and interpretations of common risk functionals.  $F_f(\ell_{f_\theta}(X, Y))$  represents the CDF of  $\ell_{f_\theta}(X, Y)$  and  $\text{VaR}_\alpha = 100 \times \alpha$ -percentile. For more discussion on these risk functionals, see Wong et al..

Risk Functional	Expression	Interpretation
Expected Value	$\mathbb{E}[\ell_{f_\theta}(X, Y)]$	expected loss
CVaR	$\mathbb{E}[\ell_{f_\theta}(X, Y)   \ell_{f_\theta}(X, Y) \geq \text{VaR}_\alpha(\ell_{f_\theta}(X, Y))]$	expectation of losses exceeding the $100 \cdot \alpha$ percentile
Inverted CVaR	$\mathbb{E}[\ell_{f_\theta}(X, Y)   \ell_{f_\theta}(X, Y) \leq \text{VaR}_\alpha(\ell_{f_\theta}(X, Y))]$	expectation of losses below the $100 \cdot \alpha$ percentile
Human-aligned	$\mathbb{E}[\ell_{f_\theta}(X, Y) w(F_f(\ell_{f_\theta}(X, Y)))]$	weighting function that overweights extreme losses
Mean-Variance	$\mathbb{E}[\ell_{f_\theta}(X, Y)] + c \cdot \text{Variance}[\ell_{f_\theta}(X, Y)]$	expected loss penalized by its variance
Trimmed Risk	$\mathbb{E}[\ell_{f_\theta}(X, Y)   F_f(\ell_{f_\theta}(X, Y)) \in [\alpha, 1 - \alpha]]$	ignore extreme losses

Table 2. Definitions and interpretation of common distribution shift settings.  $\mathbb{P}_{\text{train}}(X, Y)$  represents the joint distribution over  $X$  and  $Y$  of the training distribution.

Distribution Shift	Expression	Interpretation
General Distribution Shift	$\mathbb{P}_{\text{train}}(X, Y) \neq \mathbb{P}_{\text{test}}(X, Y)$	The training and testing distributions are not the same
Covariate Shift	$\mathbb{P}_{\text{train}}(X) \neq \mathbb{P}_{\text{test}}(X)$ , but $\mathbb{P}_{\text{train}}(Y X) = \mathbb{P}_{\text{test}}(Y X)$	Class balance changes from train to test set
Label Shift	$\mathbb{P}_{\text{train}}(Y) \neq \mathbb{P}_{\text{test}}(Y)$ , but $\mathbb{P}_{\text{train}}(X Y) = \mathbb{P}_{\text{test}}(X Y)$	A common example of this shift is noisy labels

and the model is updated with

$$\theta \leftarrow \theta - \beta \nabla_{\theta} g_{\phi} \left( \ell_{f_{\theta}}(X_{\text{train}}, Y_{\text{train}}) \right). \quad (4)$$

In summary, we minimize the following objective at each time-step

$$g_{\phi^*} \in \arg \min_{g \in \mathcal{G}} \rho \left( \ell \left( f_{\theta'}(X_{\text{val}}), Y_{\text{val}} \right) \right) \quad (5)$$

$$\text{where } f_{\theta'} \in \arg \min_{f \in \mathcal{F}} \ell \left( g_{\phi} \left( f_{\theta}(X_{\text{train}}), Y_{\text{train}} \right) \right). \quad (6)$$

Algorithm 1 details this optimization procedure in pseudocode. To point out the critical details, note that in line 6, the loss for each data point in the mini-batch is sorted from largest to smallest. Sorting from largest to smallest is not particularly important, but it is critical that the batch losses are sorted in some fashion before passing them through  $g$ . This allows for learning meaningful relations with respect to the loss magnitudes instead of the random mini-batch order. In line 8, the gradients for the learnable risk functional are dropped. This is an important implementation note, as without dropping these gradients they will be accumulated as part of the outer update, resulting in undesirable behavior (i.e. the gradients in Equation 2 will also be calculated with respect to  $\phi$  as well). Then in line 12, we use a hand-engineered risk functional  $\rho$  to calculate the validation loss. This optimization pipeline can be interpreted as learning a loss reduction functional that minimizes a desired risk on the validation set, given only information from the current mini-batch of training data.

Learning a risk functional can have an effect similar to changing learning rates. For example, if we just use  $2 * \mathbb{E}[\ell_{f_{\theta}}(X, Y)]$  as the mini-batch risk functional, then this is equivalent to using the traditional expected value but also doubling the learning rate. Therefore, we restrict our function class to be a convex combination of the loss for each data point to eliminate this effect. This comes with the additional benefit of being able to represent all of the aforementioned risk functionals (up to scaling factors) and provides straightforward interpretation. This is enforced by using the softmax of the weights of the learned risk functional linear layer. After training, the learned model is evaluated in exactly the same manner as any other model.

## 4. Experimental Evaluation

Unless otherwise noted, all experiments were performed on the CIFAR10 (Krizhevsky et al., 2009) dataset with a Resnet-18 (He et al., 2016) model. In every setting, we optimize the model for 20,000 steps, with a one-cycle learning rate schedule (Smith & Topin, 2019) that starts with a learning rate of 0.005, increasing to a maximum of 0.1, and then annealing back down to  $5e-6$ . Random cropping and flipping are used for data augmentation, and the models are trained using SGD with a momentum of 0.9, weight decay of  $5e-4$ , and a batch size of 100. These hyperparameters were selected as they were the best performing from a grid search on the hyper-validation set.

The learned mini-batch risk functionals are trained using Algorithm 1, using the same aforementioned setup, but with

Table 3. Given a risk functional to minimize (column 1), this table compares the risk achieved when optimizing a model using expected value (column 2), a model optimized with the corresponding risk functional applied per batch (column 3), a warm-started model fine-tuned with the corresponding risk functional applied per mini-batch (column 4), and a model that learns a mini-batch risk functional (column 5). The lowest-risk entries are bolded. The reported metrics are averaged over 5 runs, with the standard deviation reported in parentheses.

$\rho$	Expected Value	batch $\rho$	batch $\rho$ with warm-up	Learned
Expected Value	<b>0.2679 (0.00466)</b>	<b>0.2679 (0.00466)</b>	<b>0.2679 (0.00466)</b>	<b>0.2776 (0.00473)</b>
CVaR	2.301 (0.0317)	1.917 (0.00962)	1.773 (0.00976)	<b>1.721 (0.0156)</b>
ICVaR	1.459e-6 (1.42E-7)	8.372E-5 (3.26E-5)	1.430e-5 (1.59e-6)	<b>1.341e-7 (3.23e-8)</b>
Human	0.5953 (0.00610)	<b>0.576 (0.00762)</b>	<b>0.5753 (0.00867)</b>	0.6055 (0.0169)
Mean Var	0.3420 (0.00867)	<b>0.3288 (0.0109)</b>	<b>0.3270 (0.00332)</b>	0.3477 (0.00396)
Trimmed	0.04801 (0.00132)	<b>0.04401 (0.00153)</b>	0.05036 (0.00334)	<b>0.04602 (0.0026)</b>

Table 4. Given a risk functional to minimize (column 1), this table compares the risk of a model optimized with the corresponding risk functional applied per mini-batch (column 2), a warm-started model fine-tuned with the corresponding risk functional applied per mini-batch (column 3), and a model that learns a mini-batch risk function (column 4). The bolded entries represent the highest accuracy models. The reported metrics are averaged over 5 runs, with the standard deviation reported in parentheses.

$\rho$	batch $\rho$	batch $\rho$ w/warm-up	Learned
Expected Value	<b>91.12 (0.290)</b>	-	<b>90.76 (0.470)</b>
CVaR	68.208 (1.02)	79.14 (0.447)	<b>85.46 (0.347)</b>
ICVaR	16.78 (1.48)	89.26 (0.215)	<b>91.07 (0.0764)</b>
Human	<b>90.51 (0.141)</b>	<b>90.32 (0.416)</b>	<b>90.25 (0.530)</b>
Mean Var	<b>91.17 (0.161)</b>	90.80 (0.204)	90.75 (0.269)
Trimmed	89.05 (0.134)	89.37 (0.172)	<b>90.52 (0.149)</b>

the optimizer set to be Adam with a learning rate of 0.001 5 inner steps (Line 3 in Algorithm 1) are used, and a meta-validation batch size of 2000 (Line 10 in Algorithm 1). In all of these experiments, the risk functionals are learned in a single shot along with the model. We report the performance of each model after the metric of interest does not improve after 5 epochs, or the 20,000 step limit is reached.

In some settings, we refer to *warm-starting* a model. By warm-starting, we mean using all of the same hyperparameters mentioned above, but for 10,000 steps (including updating the learning rate schedule for this timeframe) we do normal supervised learning with the expected value risk functional. We then fine-tune the warm-started model for another 10,000 steps (again with the only change being the new annealing schedule), using the risk functional of interest. This procedure allows for the smoothest transfer between the learning objectives, produced the best results, and maintains consistency in the number of optimization steps used.

#### 4.1. Optimizing for various risk functions

We first set out to understand the mini-batch risk functionals that are uncovered when optimizing for various hand-crafted dataset risk functionals. Given a risk functional of interest (such as any from Table 1), we compare the following methods of optimizing for it: 1) train normally with expected

value as the risk functional, 2) train with the risk functional of interest applied at each mini-batch, 3) warm-start a model and then fine-tune using the risk functional applied at each mini-batch, and 4) learn a batch-level risk functional with our method. For each risk functional in Table 1, we report the average and standard deviation across 5 runs. Table 3 detail these losses, and Table 4 detail the accuracy’s.

Interestingly, in all cases, the learned mini-batch risk functional is either the best performing, or competitive with the best performing method, both in terms of loss and accuracy. Table 4 highlights the importance of warm-starting models when fine-tuning to specific risk functionals. And because our learned risk functionals are convex combinations of mini-batch losses, sorted from highest to lowest loss, there is a natural interpretation. Figures 2, 3, and 4, show the learned risk functionals from multiple points throughout training. We see that the learned risk functionals develop a curriculum that

where we see that the learned risk functionals first optimizes the model in a sort of warm-starting phase where most samples are treated equally.

However, as training further progresses, the learned risk functionals continue to become more and more specific to the setting. This automatic discovery of a warm-up period is visible in all of our learned risk functionals. Another notable



**Algorithm 1** Pseudocode for learning risk functionals.

---

**Require:** initial model parameters  $\theta$  and  $\phi$ , inner learning rate  $\beta$ , outer learning rate  $\eta$ , validation risk functional  $\rho$ , loss function without reduction  $\ell$ , a training dataset  $\mathbb{P}_{\text{train}}$ , and a validation dataset  $\mathbb{P}_{\text{val}}$

- 1: **while** not done **do**
- 2:    $f_{\theta'} = f_{\theta}$
- 3:   **for** inner steps **do**
- 4:      $X_{\text{train}}, Y_{\text{train}} \sim \mathbb{D}_{\text{train}}$  #sample batch of train data
- 5:      $\hat{y} = f_{\theta'}(X_{\text{train}})$  #Get model output
- 6:      $l_{\text{sorted}} = \text{sort}(\ell(\hat{y}, Y_{\text{train}}))$  #Compute and sort Loss
- 7:      $l = g_{\phi}(l_{\text{sorted}})$  #get risk
- 8:      $\theta' = \theta' - \beta \nabla_{\theta'} l$  #adapt  $\theta'$
- 9:   **end for**
- 10:    $X_{\text{val}}, Y_{\text{val}} \sim \mathbb{D}_{\text{val}}$  #sample validation data
- 11:    $\hat{y} = f_{\theta'}(X_{\text{val}})$  #get updated model output
- 12:    $l = \rho(\ell(\hat{y}, Y_{\text{val}}))$  #Compute validation loss
- 13:    $\phi = \phi - \eta \nabla_{\phi} l$  #Update  $\phi$
- 14:    $X_{\text{train}}, Y_{\text{train}} \sim \mathbb{D}_{\text{train}}$  #sample new train data
- 15:    $\hat{y} = f_{\theta}(X_{\text{train}})$  #get model output using original  $\theta$
- 16:    $\theta = \theta - \beta \nabla_{\theta} g_{\phi}(\ell(\hat{y}, Y_{\text{train}}))$  #update original  $\theta$
- 17: **end while**

---

finding is that the final form of the learned mini-batch risk functionals are surprisingly different from the underlying risk functional that they are optimizing for.

Here we further analyze the learned risk functionals obtained from optimizing for CVaR, ICVaR, and Trimmed Risk. In Figures 2, 3, and 4, the leftmost plot shows the risk functional that we are optimizing for (at the *dataset* level) in the same representation that we are using to display our learned mini-batch risk functions. The remainder of each row shows the *mini-batch* learned risk functional as it changes throughout training.

Figure 2 details the risk functionals resulting from optimizing for the CVaR risk functional. The CVaR risk functional focuses only on the top  $\alpha$  (in this case  $\alpha = 0.1$ ) percentile of highest losses. Or in other words, we want a model that has minimum loss on the worst (or “hardest”)  $\alpha$  percentile of the dataset. If we train a model using CVaR as the risk functional at the batch level, then we succeed in lowering the CVaR loss, but suffer a significant loss in overall accuracy ( $\sim 68\%$  accuracy down from  $\sim 91\%$ ). Introducing warm starting to this procedure further improves both the loss (by about 7.5%) and the accuracy (by about 16% relative) of the learned model. However, if we allow the mini-batch risk function to be learned, we get further improvement in both the loss and the accuracy (relative improvements over the risk function of 10% and 25% respectively). Inspecting the learned mini-batch risk function (Figure 2), we see that near the end of the training, the gradients from only the highest loss samples are kept, although not treated equally

(with the most weight given to the highest loss sample, tapering off from there). Again, we see that the model has learned a sort of warm-up schedule, where earlier in training, all samples are treated relatively similarly, and then the weighting is slowly shifted towards the high-loss samples as training progresses. Of further note is the smoothness from which the learned mini-batch risk function transitions out of the warm-up phase, vs a more sudden transition caused by hand-engineered warm-up schedules.

We see similar results when learning mini-batch risk functions for the ICVaR risk. In this case, we are again using  $\alpha = 0.1$ , meaning that the loss we want to minimize is the loss on the lowest loss (“easiest”) 10% of data. Namely, we again see the best-performing method being the learned risk functional both in terms of loss and accuracy (with relative improvements over the risk functional with and without warm-up of 2% and 99% respectively). But more interestingly, we find that the learned risk functional responsible for this reduction in loss, while also improving accuracy, differs drastically from the ICVaR risk functional, as shown in Figure 3. Again, warm-up schedule behavior is shown, and initially, more weight is placed on the lowest-loss samples as we would expect. However, as training progresses, more weight is placed on the middle quantiles of losses. This seems to be in light of the fact that using just the lowest 10% of losses in each mini-batch to train with yields an extremely poor model ( $\sim 17\%$  accuracy as shown in Table 4). Therefore, information from higher-loss samples is still beneficial to model optimization and risk reduction, even when only focusing on the “easiest” subset of the data.

The learned mini-batch risk functional for optimizing the trimmed risk again starts with a warm-up-like period before converging on a trimmed-risk-like risk functional, but, also again, biased towards the higher losses. We continue to use  $\alpha = 0.1$ , indicating that we discard the loss from the highest and lowest 10% of the data. In all of the learned risk functionals, the transition point between samples that are given high vs low weight is much smoother than that of the risk functional being optimized.

## 4.2. Learning Mini-Batch Risk Functionals for Label Noise

Now that we have demonstrated the effectiveness of our method in finding useful mini-batch risk functionals, we explore its applicability to a specific distribution shift: label noise. In this section, we introduce different levels of label noise to the CIFAR10 dataset, and then explore the different models learned with and without a mini-batch learned risk functional. To induce noise, we randomly select a percentage of the training data, and then reassign labels uniformly at random. We first explore the models learned when given access to the noisy data along with a small, noise-free, sub-

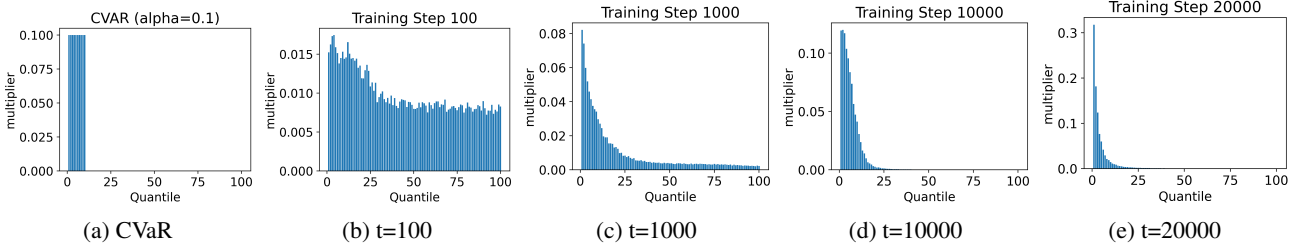


Figure 2. Visualizations of the mini-batch risk functional learned when optimizing for the CVaR ( $\alpha = 0.1$ ) risk of the CIFAR-10 dataset, using a Resnet-18 model. Subfigure 2a indicates the dataset-level risk functional we are optimizing for, and the remaining figures are the learned mini-batch risk functionals at different training time steps (indicated by the subfigure caption). The y-axis indicates the multiplier applied to the corresponding quantile (sorted by magnitude) of each batch. The left side of each plot corresponds to the largest loss in the mini-batch, and the right side of each plot corresponds to the smallest loss in the mini-batch. The learned mini-batch risk functional learns a warm-up schedule before finally focusing on the highest loss samples.

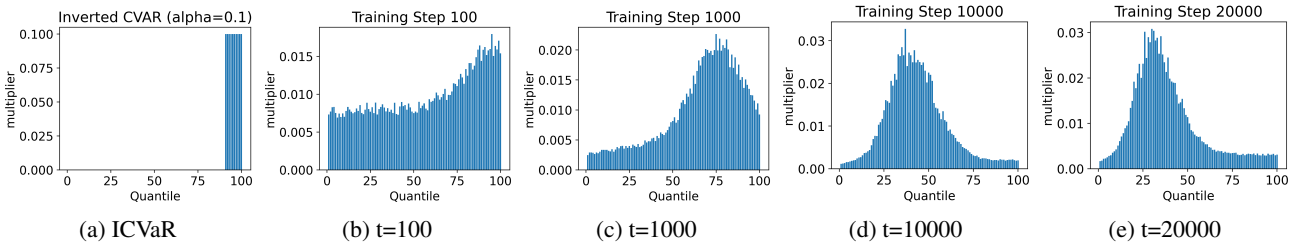


Figure 3. Visualizations of the mini-batch risk functional learned when optimizing for the ICVaR ( $\alpha = 0.1$ ) risk of the CIFAR-10 dataset, using a Resnet-18 model. Subfigure 3a indicates the dataset-level risk functional we are optimizing for, and the remaining figures are the learned risk functional at different training time steps (indicated by the subfigure caption). The y-axis indicates the multiplier applied to the corresponding quantile (sorted by magnitude) of each mini-batch. The left side of each plot corresponds to the largest loss in the mini-batch, and the right side of each plot corresponds to the smallest loss in the mini-batch. The learned risk functional learns a warm-up schedule, and although initially focusing on the lower mini-batch losses, the emphasis is placed more on middle quantiles of losses later in training, although the ICVaR loss penalizes only the lowest loss samples.

set of 1,000 samples (2% of the training set). Then, more interestingly, we demonstrate that the performance of our method suffers only very minor degradation when a noise-free subset is not present.

Table 5 shows the accuracy when training a model with and without a learned mini-batch risk functional, given a noise-free validation set of 1,000 samples. As the noise becomes more drastic, the benefit of a learned risk functional increases. Notably, even when no label noise is present, using a learned mini-batch risk functional reaches *equal* accuracy to that of a model trained normally. At 5% label noise, a learned mini-batch risk function improves accuracy by  $\sim 1.7\%$  absolute, whereas at 50% label noise, this improvement is  $\sim 8.6\%$  absolute.

Conventional wisdom is that the correct thing to do when learning with a known level of 50% label noise is to train a model with the ICVaR functional with  $\alpha = 0.5$ . This would tell the model to focus only on the lowest 50% of losses in the dataset, therefore ignoring the mislabeled 50% (with the assumption that the mislabeled data points have higher

loss than correctly labeled data points). However, as indicated from the results in Table 4, warm-starting is critical to training effective models with ICVaR (and warm-starting makes the aforementioned assumption likely to hold). As the results from Table 4 further demonstrate, simply training with this risk functional applied at the mini-batch does not always produce the best results. Although our method *does not* have access to information such as the amount of noise in the dataset, or even the type of distribution shift present, we compare against an *Oracle* model that is given all of this information and therefore can be optimally trained. These results are added under the Oracle column in Table 6.

The mini-batch risk functional learned when 50% label noise is present is shown in Figure 5 (note that at 50% random labels, there is a chance that each label is randomly assigned the proper label - resulting in a true level of label noise around 45%). Interestingly, we again see the automatically learned warm-up behavior, but the learned mini-batch risk functional resembles the ICVaR functional only in part. While the latter percentiles of loss are similar (roughly the

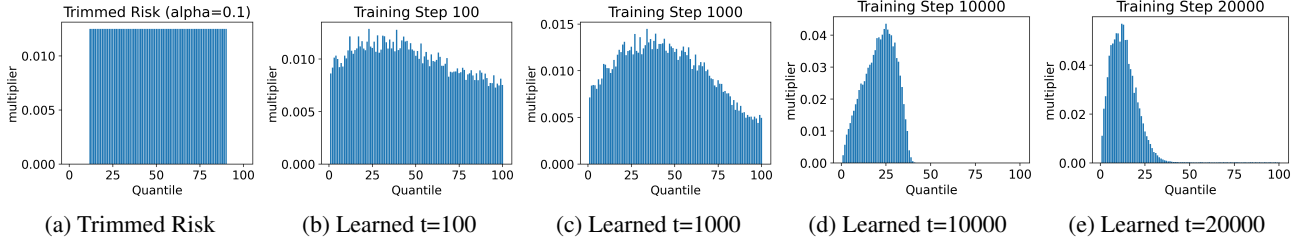


Figure 4. Visualizations of the mini-batch risk functional learned when optimizing for the trimmed risk (at  $\alpha = 0.1$ ) of the CIFAR-10 dataset, using a Resnet-18 model. Subfigure 4a indicates the dataset-level risk functional we are optimizing for, and the remaining figures are the learned risk functional at different training time steps (indicated by the subfigure caption). The y-axis indicates the multiplier applied to the corresponding quantile (sorted by magnitude) of each mini-batch. The left side of each plot corresponds to the largest loss in the mini-batch, and the right side of each plot corresponds to the smallest loss in the mini-batch. The learned risk functional learns a warm-up schedule, and although initially focusing most on the middle quantiles of losses (as expected because of the trimmed risk functional), the learned mini-batch risk functional focuses more on the higher loss samples later in training.

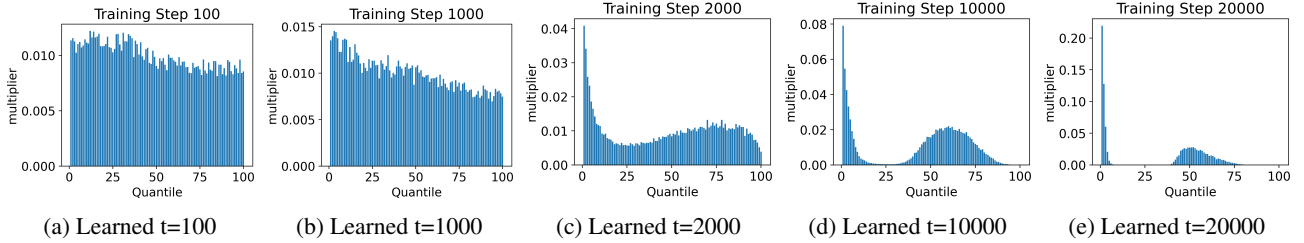


Figure 5. Visualizations of the mini-batch risk functional learned when optimizing for the expected value of the validation loss of the CIFAR-10 dataset with 50% random labels, using a Resnet-18 model. Each figure represents the learned mini-batch risk functional at different training time steps (indicated by the subfigure caption). The y-axis indicates the multiplier applied to the corresponding quantile (sorted by magnitude) of each batch. The left side of each plot corresponds to the largest loss in the batch, and the right side of each plot corresponds to the smallest loss in the batch. The learned risk functional learns a warm-up schedule, and then begins to down weight most of the high-loss samples (except for the very highest losses) and focus more on the lower-loss quantiles. Surprisingly, even late in training, the focus on the lower quantiles remains, but so does the emphasis on a small number of high-loss samples.

50th to 75th percentile), it places high emphasis on a few of the highest-loss samples. This emphasis on high-loss samples is surprising, even though the emphasis on them becomes less throughout training.

## 5. Related Work

Several studies have focused on understanding how to optimize for risk functionals other than the average (Duchi & Namkoong, 2021; Duchi et al., 2022). Furthermore, Leqi et al. (2019) showed that the minimization of risk functionals *other than* the expected loss is beneficial with respect to some desiderata such as fairness, and for better aligning with a more human-like risk measure. In Li et al. (2020), a hand-engineered functional for determining the weight for each sample in a mini-batch is presented, and display its effectiveness in enforcing fairness, mitigating outliers, and handling class imbalance. They show that this sample weighting scheme can adapt to new applications such as simultaneously addressing outliers and promoting fairness.

While we present a method for learning risk functionals in any setting, one related application that has received much attention is learning with noisy labels. Although we focus on the more general setting, here we include some of the most related work in this subfield. After it was proven that a deep neural network with a modified loss function for noisy data can approach the Bayes optimal classifier (Manwani & Sastry, 2013; Ghosh et al., 2017), many efforts at hand-engineering more robust loss functionals followed. These include generalized gross entropy (Zhang & Sabuncu, 2018), Bi-tempered loss (Amid et al., 2019), and 0-1 loss surrogate loss functionals that can ignore samples, based on a threshold Lyu & Tsang (2019). While these have shown benefits in specific settings, they have not been adopted for more general use. Our work extends this by learning a sample weighting function instead of relying on hand engineering.

Estimation of a noise transition matrix is also common in learning with noisy labels. The noise transition matrix is then used to transform model outputs from a noiseless to

Table 5. This table compares learning among label noise when also given access to a noise-free validation set of 1,000 samples (2% of the training set). Column 1 indicates the percentage of the training labels that were randomly assigned, column 2 indicates the baseline test accuracy of training with the expected value, and column 3 shows the accuracy when training with a learned risk functional. We also trained a model only on the clean data, which achieves an accuracy of 61.21% (1.712).

% Random Labels	Expected Value	Learned Risk Function
0%	<b>91.25 (0.241)</b>	<b>91.08 (0.277)</b>
5%	80.98 (0.161)	<b>82.65 (0.549)</b>
20%	71.75 (0.909)	<b>79.02 (0.4807)</b>
50%	60.18 (2.94)	<b>68.75 (1.42)</b>

Table 6. This table compares learning among label noise, but without access to a noise-free validation set. Column 1 indicates the percentage of the training labels that were randomly assigned, column 2 indicates the baseline test accuracy of training with the expected value, column 3 shows the accuracy when training with a learned mini-batch risk functional, and column 4 shows the oracle accuracy. The oracle is given information such as the optimal risk functional and corresponding parameters to use, which is typically not available.

Random Labels	Expected Value	Learned Risk Function	Oracle
0%	<b>91.25 (0.241)</b>	<b>91.08 (0.277)</b>	-
5%	80.62 (0.498)	<b>81.71 (0.289)</b>	84.07 (0.189)
20%	68.46 (0.394)	<b>77.85 (0.557)</b>	82.31 (0.376)
50%	60.72 (2.46)	<b>69.54 (1.23)</b>	76.86 (0.311)

noisy label domain (Patrini et al., 2017; Hendrycks et al., 2018; Yao et al., 2020; Yang et al., 2021). Similarly, Xiao et al. (2015); Han et al. (2018); Yao et al. (2018) build network architectures specific for learning among label noise. These methods focus on mapping from model output to noise-adapted posterior, whereas we learn a reduction function that maps from batch losses to reduced batch loss.

Another interpretation of our method is that it is a form of importance weighting. Liu & Tao (2015) apply importance weighting to learning with noisy labels. They present a method of estimating the target and source distribution labels using kernel density estimation. Wang et al. (2017) also apply importance weighting in this setting, by modifying the updates according to an estimate of the proportion of randomly labeled examples. Chang et al. (2017) follow this setting as well, but their updates are modified according to the variance in predicted probabilities of the correct class across mini-batches. Again, our method goes beyond these by learning a weighting function from a much larger function class (i.e. more expressive function classes), and in

that it operates as a loss reduction strategy leveraging only information available in a batch of data.

Jenni & Favaro (2018) introduce bi-level optimization that learns a function that assigns a scalar weight to the batch loss. More specifically, given a clean validation set, each mini-batch is weighted according to how well its gradient aligns with one calculated on clean data. In contrast, our method learns to weight each sample in a batch before reduction and does not require clean data. Meta-weight-net (Shu et al., 2019) learns a function that scales the loss of every sample in a batch (independent of the other samples in the batch - a sample producing the same loss in multiple batches will be scaled equally to the same value). Ren et al. (2018) also learn a reduction function that maps from batch losses to reduced batch loss via a meta-learning-inspired update. Our method differs from these two works by being sensitive to the relative performance of samples within each batch (achieved by enforcing sorting and then scaling the loss of each sample with respect to their ranking in the batch - the same loss in different batches are treated differently) instead of the loss value itself, and by allowing flexibility in the number of inner steps (i.e. more exact approximations).

Shen & Sanghavi (2019) minimize the trimmed loss by alternating between selecting true-labeled examples and retraining a model. At each round, they keep only a fraction of small-loss examples to retrain the model during the next round. In contrast, we learn our risk functionals in a single shot. Lastly, as we will demonstrate in Section 4.2, our method does not depend on having a clean validation set. We are not aware of any work that presents a general-use method for learning mini-batch risk functionals.

## 6. Conclusion

We introduced a meta-learning-based method of learning an interpretable mini-batch risk functional during model training, in a single shot, that both outperforms hand-engineered risk functionals and discovers useful mini-batch risk functionals in settings where they are unknown a priori. When optimizing for various risk functionals, the learned mini-batch risk functions lead to risk reduction of up to 10% over hand-engineered ones. Then in the presence of label noise, where risk functionals can be useful but the right one is unknown, our method improved over baseline by over 14% relative ( $\sim 9\%$  absolute) among 50% random labels, even when given *no* noise-free data. Our learned mini-batch risk functions are restricted to taking a convex combination of mini-batch loss quantiles, and are therefore clearly interpretable. We analyzed the learned mini-batch risk functionals at different points through training, and found that they learned curriculums (including warm-up periods), and that their final form can be surprisingly different from the underlying risk functional that they optimized for.



## References

- Amid, E., Warmuth, M. K., Anil, R., and Koren, T. Robust bi-tempered logistic loss based on bregman divergences. *Advances in Neural Information Processing Systems*, 32, 2019.
- Busmann, N., Giudici, P., Marinelli, D., and Papenbrock, J. Explainable machine learning in credit risk management. *Computational Economics*, 57(1):203–216, 2021.
- Chang, H.-S., Learned-Miller, E., and McCallum, A. Active bias: Training more accurate neural networks by emphasizing high variance samples. *Advances in Neural Information Processing Systems*, 30, 2017.
- Duchi, J., Hashimoto, T., and Namkoong, H. Distributionally robust losses for latent covariate mixtures. *Operations Research*, 2022.
- Duchi, J. C. and Namkoong, H. Learning models with uniform performance via distributionally robust optimization. *The Annals of Statistics*, 49(3):1378–1406, 2021.
- Finn, C., Abbeel, P., and Levine, S. Model-agnostic meta-learning for fast adaptation of deep networks. In *International conference on machine learning*, pp. 1126–1135. PMLR, 2017.
- Ghosh, A., Kumar, H., and Sastry, P. S. Robust loss functions under label noise for deep neural networks. In *Proceedings of the AAAI conference on artificial intelligence*, volume 31, 2017.
- Han, B., Yao, J., Niu, G., Zhou, M., Tsang, I., Zhang, Y., and Sugiyama, M. Masking: A new perspective of noisy supervision. *Advances in neural information processing systems*, 31, 2018.
- He, K., Zhang, X., Ren, S., and Sun, J. Deep residual learning for image recognition. In *Proceedings of the IEEE conference on computer vision and pattern recognition*, pp. 770–778, 2016.
- Hendrycks, D., Mazeika, M., Wilson, D., and Gimpel, K. Using trusted data to train deep networks on labels corrupted by severe noise. *Advances in neural information processing systems*, 31, 2018.
- Hoffman, M., Kahn, L. B., and Li, D. Discretion in hiring. *The Quarterly Journal of Economics*, 133(2):765–800, 2018.
- Jenni, S. and Favaro, P. Deep bilevel learning. In *Proceedings of the European Conference on Computer Vision (ECCV)*, September 2018.
- Krizhevsky, A., Hinton, G., et al. Learning multiple layers of features from tiny images. 2009.
- Kruppa, J., Schwarz, A., Arminger, G., and Ziegler, A. Consumer credit risk: Individual probability estimates using machine learning. *Expert systems with applications*, 40(13):5125–5131, 2013.
- Leqi, L., Prasad, A., and Ravikumar, P. K. On human-aligned risk minimization. *Advances in Neural Information Processing Systems*, 32, 2019.
- Li, T., Beirami, A., Sanjabi, M., and Smith, V. Tilted empirical risk minimization. *arXiv preprint arXiv:2007.01162*, 2020.
- Liu, T. and Tao, D. Classification with noisy labels by importance reweighting. *IEEE Transactions on pattern analysis and machine intelligence*, 38(3):447–461, 2015.
- Lyu, Y. and Tsang, I. W. Curriculum loss: Robust learning and generalization against label corruption. *arXiv preprint arXiv:1905.10045*, 2019.
- Manwani, N. and Sastry, P. Noise tolerance under risk minimization. *IEEE transactions on cybernetics*, 43(3):1146–1151, 2013.
- Patel, B. N., Rosenberg, L., Willcox, G., Baltaxe, D., Lyons, M., Irvin, J., Rajpurkar, P., Amrhein, T., Gupta, R., Halabi, S., et al. Human-machine partnership with artificial intelligence for chest radiograph diagnosis. *NPJ digital medicine*, 2(1):1–10, 2019.
- Patrini, G., Rozza, A., Krishna Menon, A., Nock, R., and Qu, L. Making deep neural networks robust to label noise: A loss correction approach. In *Proceedings of the IEEE conference on computer vision and pattern recognition*, pp. 1944–1952, 2017.
- Raghavan, M., Barocas, S., Kleinberg, J., and Levy, K. Mitigating bias in algorithmic hiring: Evaluating claims and practices. In *Proceedings of the 2020 conference on fairness, accountability, and transparency*, pp. 469–481, 2020.
- Rajpurkar, P., O’Connell, C., Schechter, A., Asnani, N., Li, J., Kiani, A., Ball, R. L., Mendelson, M., Maartens, G., van Hoving, D. J., et al. Chexaid: deep learning assistance for physician diagnosis of tuberculosis using chest x-rays in patients with hiv. *NPJ digital medicine*, 3(1):1–8, 2020.
- Ren, M., Zeng, W., Yang, B., and Urtasun, R. Learning to reweight examples for robust deep learning. In *International conference on machine learning*, pp. 4334–4343. PMLR, 2018.
- Shen, Y. and Sanghavi, S. Learning with bad training data via iterative trimmed loss minimization. In

- Chaudhuri, K. and Salakhutdinov, R. (eds.), *Proceedings of the 36th International Conference on Machine Learning*, volume 97 of *Proceedings of Machine Learning Research*, pp. 5739–5748. PMLR, 09–15 Jun 2019. URL <https://proceedings.mlr.press/v97/shen19e.html>.
- Shu, J., Xie, Q., Yi, L., Zhao, Q., Zhou, S., Xu, Z., and Meng, D. Meta-weight-net: Learning an explicit mapping for sample weighting. *Advances in neural information processing systems*, 32, 2019.
- Smith, L. N. and Topin, N. Super-convergence: Very fast training of neural networks using large learning rates. In *Artificial intelligence and machine learning for multi-domain operations applications*, volume 11006, pp. 369–386. SPIE, 2019.
- Tschandl, P., Rinner, C., Apalla, Z., Argenziano, G., Codella, N., Halpern, A., Janda, M., Lallas, A., Longo, C., Malvehy, J., et al. Human–computer collaboration for skin cancer recognition. *Nature Medicine*, 26(8):1229–1234, 2020.
- Wang, R., Liu, T., and Tao, D. Multiclass learning with partially corrupted labels. *IEEE transactions on neural networks and learning systems*, 29(6):2568–2580, 2017.
- Wong, W., Huang, A., Leqi, L., Azizzadenesheli, K., and Lipton, Z. C. Riskyzoo: A library for risk-sensitive supervised learning.
- Xiao, T., Xia, T., Yang, Y., Huang, C., and Wang, X. Learning from massive noisy labeled data for image classification. In *Proceedings of the IEEE conference on computer vision and pattern recognition*, pp. 2691–2699, 2015.
- Yang, S., Yang, E., Han, B., Liu, Y., Xu, M., Niu, G., and Liu, T. Estimating instance-dependent label-noise transition matrix using dnns. *arXiv preprint arXiv:2105.13001*, 2021.
- Yao, J., Wang, J., Tsang, I. W., Zhang, Y., Sun, J., Zhang, C., and Zhang, R. Deep learning from noisy image labels with quality embedding. *IEEE Transactions on Image Processing*, 28(4):1909–1922, 2018.
- Yao, Y., Liu, T., Han, B., Gong, M., Deng, J., Niu, G., and Sugiyama, M. Dual t: Reducing estimation error for transition matrix in label-noise learning. *Advances in neural information processing systems*, 33:7260–7271, 2020.
- Zhang, Z. and Sabuncu, M. Generalized cross entropy loss for training deep neural networks with noisy labels. *Advances in neural information processing systems*, 31, 2018.